Metal Modulation and KDM Inhibition Restores Retinal Function in a Zebrafish Model of Age-Related Retinal Degeneration

Itzchak Angel *, Kalaichitra Periyasamy, Micha Gladnikoff, Benin Joseph, Raphael Mayer, Erez Aminov

Posted Date: 10 July 2026

doi: 10.20944/preprints202607.0729.v1

Keywords: retinal degeneration; age-related macular degeneration; JmjC histone demethylases; KDM inhibition; epigenetic reprogramming; intracellular metal modulation; oxidative stress; zebrafish model

 doi:10.20944/preprints202607.0729.v1

Article

Metal Modulation and KDM Inhibition Restores Retinal Function in a Zebrafish Model of Age-Related Retinal Degeneration

Itzchak Angel [1,*], Kalaichitra Periyasamy [2], Micha Gladnikoff [3], Benin Joseph [2], Raphael Mayer [3] and Erez Aminov [1]

[1] Telomir Pharmaceuticals, Inc., Miami, FL, USA
[2] Pentagrit Discovery Lab, Chennai, Tamil Nadu, India
[3] Smart Assays Biotechnologies, Nes Ziona, Israel
* Correspondence: angel@telomirpharma.com

Abstract

Retinal degeneration is associated with mitochondrial dysfunction, oxidative stress, and disruption of metal homeostasis within the retinal pigment epithelium (RPE). Dysregulation of redox-active metals has been implicated in age-related macular degeneration (AMD), but whether targeted intracellular metal modulation preserves retinal structure and function remains unclear. This study explores the effect of metal ion modulation on retinal structure and visual function. Telomir-Zn, a first-in-class intracellular metal modulator, depletes labile Fe^{2+}, potently inhibits multiple JmjC KDMs, and induces epigenetic reprogramming. In a zebrafish model combining impaired DNA repair and mitochondrial dysfunction ($Sen57^{wrn-/-}ND6^{-/+}$), Telomir-Zn reduced oxidative stress, preserved retinal architecture, improved visual behaviors, and partially normalized telomeric content and CpG methylation patterns. Complementary studies in human ARPE-19 RPE cells showed attenuation of iron/copper-induced ROS and calcium dysregulation, with reciprocal zinc accumulation and labile Fe^{2+} depletion. These findings establish targeted metal modulation and multi-KDM inhibition as a novel strategy to mitigate oxidative-epigenetic stress and preserve retinal structure/function in degenerative disease, supporting further development for AMD.

Keywords: retinal degeneration; age-related macular degeneration; JmjC histone demethylases; KDM inhibition; epigenetic reprogramming; intracellular metal modulation; oxidative stress; zebrafish model

1. Introduction

Retinal degeneration is characterized by mitochondrial dysfunction, oxidative stress, and impaired cellular homeostasis, particularly within the RPE—key features of AMD. Dysregulation of redox-active metals (iron and copper) promotes ROS generation via Fenton chemistry and contributes to lipid peroxidation, inflammation, and photoreceptor loss.

The retina is uniquely vulnerable to oxidative injury because of its high metabolic demand, oxygen consumption, and lipid-rich environment. Increasing evidence implicates dysregulation of redox-active transition metals, particularly iron and copper, as contributors to oxidative damage in the retina and RPE. Excess labile iron has been associated with lipid peroxidation, mitochondrial dysfunction, inflammatory signaling, and photoreceptor loss in experimental models and human AMD [1–4].

Iron and copper are essential for retinal physiology, serving critical roles in electron transport and enzymatic activity. However, when present in excess or improperly compartmentalized, these metals promote ROS generation through redox cycling and Fenton chemistry [5,6]. Oxidative stress and mitochondrial dysfunction influence chromatin regulation and genomic stability in retinal cells.

 doi:10.20944/preprints202607.0729.v1

Fe^{2+}-dependent Jumonji C (JmjC) histone demethylases (KDM2, KDM5, KDM6 families) serve as critical sensors of intracellular metal and redox status. These enzymes regulate chromatin accessibility and expression of genes involved in inflammation, senescence, DNA repair, and cell survival [7–10]. Dysregulated KDM activity links metal imbalance to epigenetic alterations that exacerbate retinal degeneration. Zinc, in contrast, acts as a redox-inert structural cofactor for transcription factors and repair proteins.

Zinc represents a functionally distinct metal within this context. Unlike iron and copper, zinc is redox-inert under physiological conditions yet serves as an essential structural cofactor for numerous transcription factors, DNA repair proteins, and chromatin-associated complexes [11–13]. Intracellular zinc homeostasis is tightly regulated and intersects with iron metabolism through shared buffering and transport mechanisms. Disruption of zinc–iron balance has been associated with increased oxidative stress and impaired genomic stability in aging tissues, but its contribution to retinal degeneration remains incompletely defined.

The zebrafish (Danio rerio) provides a vertebrate system well suited for investigating retinal oxidative pathology because of its conserved retinal architecture, optical accessibility, and established models of retinal degeneration [14–17]. Zebrafish lines combining mitochondrial dysfunction and impaired DNA repair exhibit accelerated retinal degeneration characterized by photoreceptor loss, RPE disruption, elevated ROS, and visual impairment [18–20], recapitulating key features of oxidative retinal disease.

Telomir-Zn modulates intracellular metal pools (preferential $Cu^{2+} > Fe^{2+}$ affinity), depletes labile Fe^{2+}, and potently inhibits multiple JmjC KDMs. This study evaluates whether such modulation preserves retinal integrity in a zebrafish model of accelerated oxidative retinal degeneration while providing mechanistic insights into metal-KDM-epigenetic axes.

Using a zinc-based intracellular metal modulator, we evaluated effects on retinal architecture, visual behavior, oxidative stress, and genomic regulatory measures. Complementary experiments in human RPE cells examined whether intracellular metal redistribution alters redox-active metal pools and attenuates iron- and copper-induced oxidative stress. Together, these studies evaluate whether targeted intracellular metal regulation can stabilize redox balance and preserve retinal integrity in vivo.

2. Results

2.1. Metal-Dependent Modulation Attenuates Oxidative Stress and Calcium Dysregulation in Human Retinal Cells

Oxidative stress disrupts intracellular calcium homeostasis through release of calcium from mitochondria and other intracellular stores. To determine whether modulation of intracellular metal balance influences metal-induced calcium dysregulation, ARPE-19 retinal pigment epithelial cells were challenged with Fe^{2+} or Cu^{2+}, and intracellular calcium flux was quantified using the calcium-sensitive fluorescent probe Fluo-8.

Exposure to Fe^{2+} (10 μM) induced a pronounced increase in intracellular calcium flux. Treatment with Telomir-Zn produced a dose-dependent attenuation of this response (Figure 1A). Similarly, Cu^{2+} challenge (25 μM) triggered a delayed but sustained elevation in intracellular calcium levels between 10 and 20 minutes, which was markedly reduced in the presence of Telomir-Zn across tested concentrations (Figure 1B).

Intracellular ROS levels were quantified using DCFH-DA fluorescence. Copper exposure resulted in a robust increase in ROS. Telomir-Zn reduced baseline oxidative stress and dose-dependently reversed copper-induced ROS accumulation, restoring ROS levels toward baseline at concentrations as low as 1 μM (Figure 1C).

 doi:10.20944/preprints202607.0729.v1

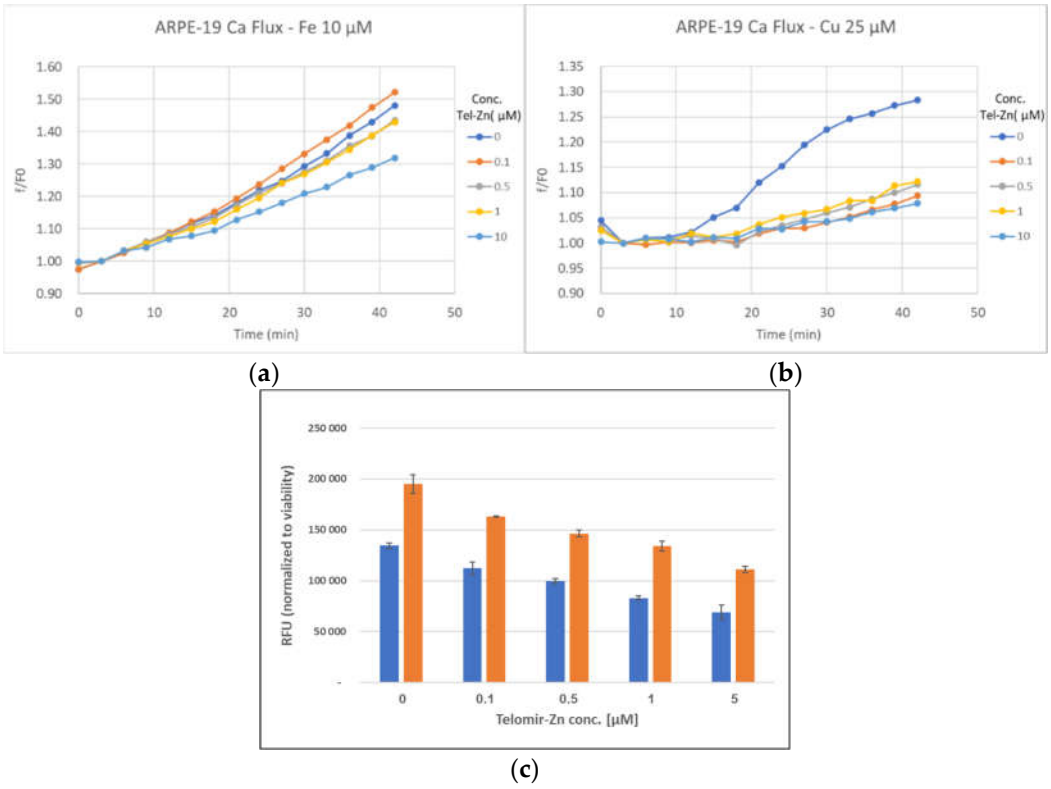

Figure 1. Metal-dependent modulation attenuates calcium dysregulation and oxidative stress in ARPE-19 cells. (**A**) Intracellular calcium flux in ARPE-19 cells following exposure to Fe^{2+} (10 µM) in the presence or absence of Telomir-Zn (0.1–5 µM). (**B**) Intracellular calcium flux following Cu^{2+} (25 µM) exposure with or without Telomir-Zn. (**C**) Intracellular reactive oxygen species (ROS) levels measured using 2′,7′-dichlorofluorescein diacetate (DCFH-DA) fluorescence following copper exposure. Data are presented as mean ± standard deviation (SD). Statistical analysis was performed using one-way analysis of variance (ANOVA) followed by Tukey's multiple-comparisons post hoc test.

2.2. Reciprocal Intracellular Zinc Accumulation and Labile Iron Depletion

To determine whether modulation of intracellular metal homeostasis alters labile metal pools, intracellular zinc and ferrous iron levels were quantified in a model cellular system, using cultured human HaCaT cells with complementary fluorescent probes. Labile zinc was measured using DA-ZP1, and redox-active ferrous iron (Fe^{2+}) was assessed using FerroOrange.

Short-term exposure to Telomir-Zn induced a rapid, dose-dependent increase in intracellular zinc fluorescence, detectable within 30 minutes and sustained for at least 2 hours (Figure 2A). Zinc accumulation was observed at concentrations as low as 0.1–1 µM without detectable effects on cell confluence or viability.

In parallel, FerroOrange staining demonstrated a reciprocal decrease in intracellular labile Fe^{2+} levels across the same concentration range (Figure 2B). Increasing Telomir-Zn concentrations were associated with progressive suppression of FerroOrange fluorescence.

 doi:10.20944/preprints202607.0729.v1

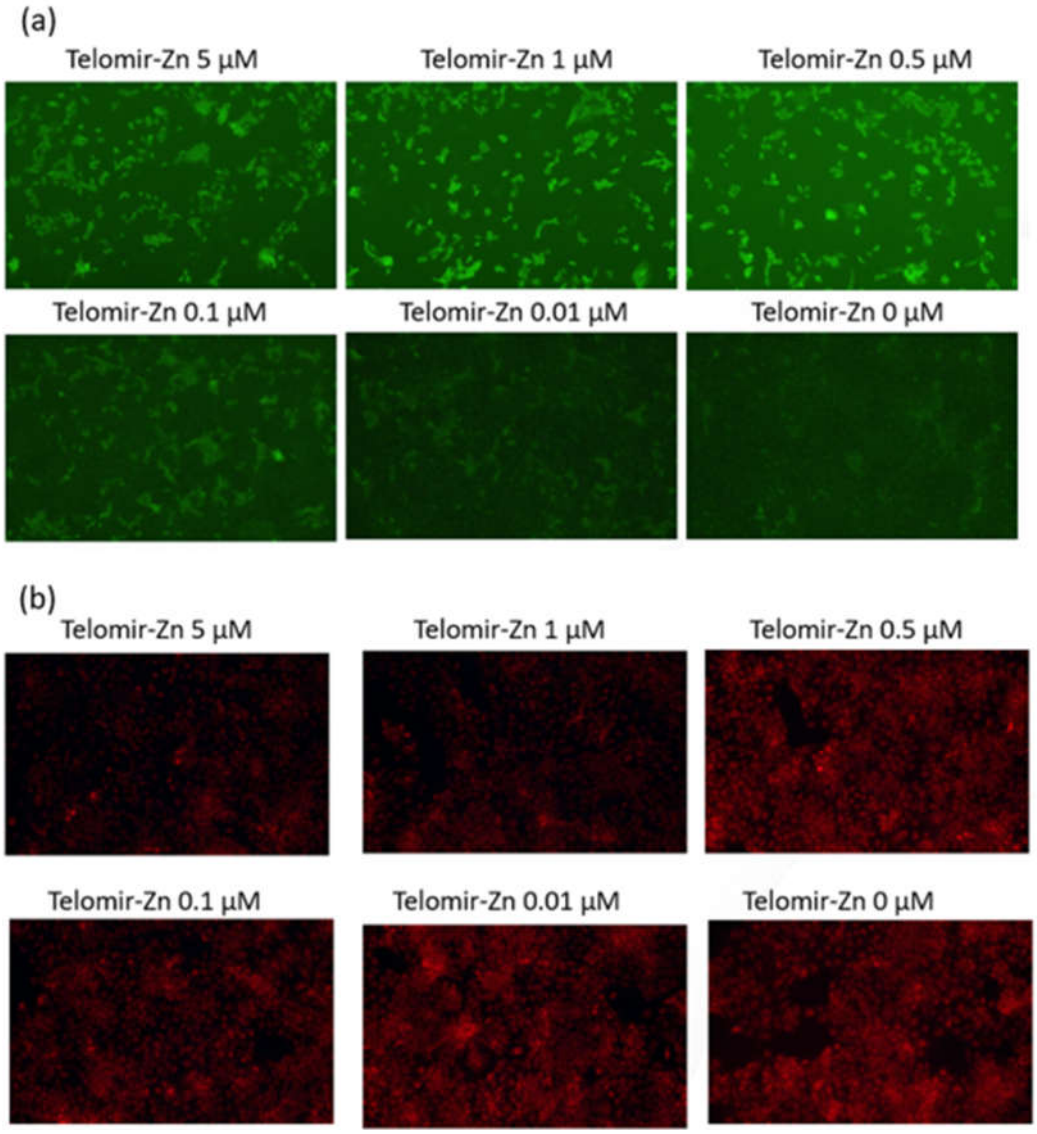

Figure 2. Reciprocal intracellular zinc accumulation and labile iron depletion following metal modulation. (**A**) Representative fluorescence microscopy images of HaCaT cells stained with the zinc-selective probe DA-ZP1 following 2-hour incubation with increasing concentrations of Telomir-Zn (0.01–5 µM). (**B**) Representative fluorescence images of FerroOrange staining demonstrating intracellular labile ferrous iron (Fe^{2+}) levels following 2-hour Telomir-Zn exposure. Images were acquired at 10× magnification. Quantification was performed using biologically independent samples.

2.3. Telomir-Zn Potently Inhibits JmjC Histone Demethylases

Biochemical assays demonstrated low-nanomolar potency of Telomir-Zn against key KDM family members (Table 1; Figure S1). Strongest inhibition was observed for KDM5B (63 nM), followed by KDM2A (240 nM), KDM5A (310 nM), KDM2B (300 nM), KDM6A (390 nM), KDM5C (470 nM), and KDM6B (2000 nM). This multi-KDM blockade is expected to promote accumulation of activating histone marks and reduce aberrant DNA methylation at stress-response loci (Table 1).

Table 1. Inhibitory Potency of Telomir-Zn Against JmjC Histone Demethylases (KDMs).

KDM Family	Specific Enzyme (Alias)	Primary Methylation Target(s)	Telomir-Zn Effect IC_{50}, nM
KDM2	KDM2A (FBXL11)	H3K36me2	240
	KDM2B (FBXL10)		300

 doi:10.20944/preprints202607.0729.v1

KDM6	KDM6A (UTX)	H3K27me3	390
	KDM6B (JMJD3)		2000
KDM5	KDM5A (JARID1A)	H3K4me3/H3K4me2	310
	KDM5B (JARID1B)		63
	KDM5C (JARID1C)		470

2.4. Zebrafish Studies

2.4.1. Improvement in Visual Performance

Sen57$^{wrn-/-}$ND6$^{-/+}$ zebrafish exhibited prolonged central visual response latency compared with WT controls (49.9 ± 4.9 s versus 0.5 ± 0 s; $P < 0.0001$). Telomir-Zn reduced latency in a dose-dependent manner (Figure 3A).

The degeneration model also demonstrated delayed moving object response and light adaptation latencies relative to WT animals ($P < 0.0001$). Treatment significantly reduced response latency at both doses, with greater improvement observed at the higher dose (Figure 3B,C).

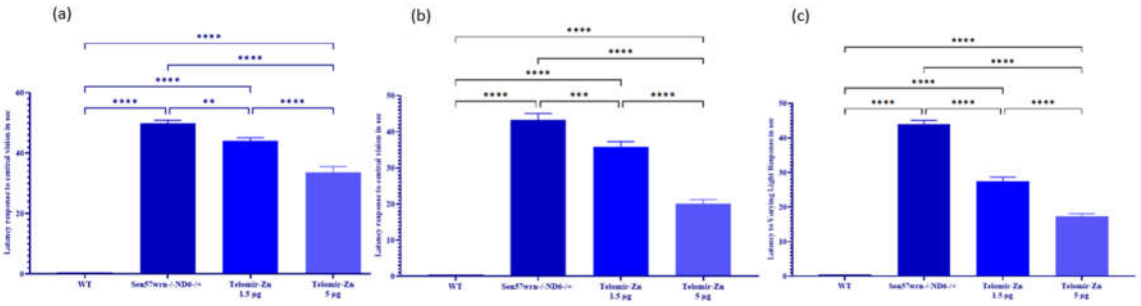

Figure 3. Metal-dependent modulation improves visual response latency in Sen57$^{wrn-/-}$ND6$^{-/+}$ zebrafish. (**A**) Latency to central visual response. (**B**) Latency to moving object tracking response. (**C**) Latency to variable light adaptation response. Data are presented as mean ± SD (n = 24 per group). Statistical analysis was performed using one-way ANOVA followed by Tukey's multiple-comparisons post hoc test.

2.4.2. Retinal Structural Preservation

Histological examination revealed intact laminar retinal organization in wild-type zebrafish, whereas Sen57$^{wrn-/-}$ND6$^{-/+}$ animals exhibited pronounced retinal degeneration characterized by photoreceptor loss, thinning of the outer nuclear layer (ONL), disruption of the RPE, and disorganization of inner retinal layers.

Quantitative analysis demonstrated a significant increase in retinal degeneration in the accelerated aging model compared with wild-type controls (14.5 ± 6.7% versus 0%; $P < 0.001$). Treated animals showed restoration of ONL, INL, OPL, and GCL thickness, indicative of structural stabilization and regenerative remodeling of retinal layers. Modulation of intracellular metal homeostasis significantly reduced the extent of retinal degeneration. Both doses produced a similar, significant reduction in degenerative burden ($P < 0.05$ versus model), indicating important stabilization of retinal architecture (Figure 4).

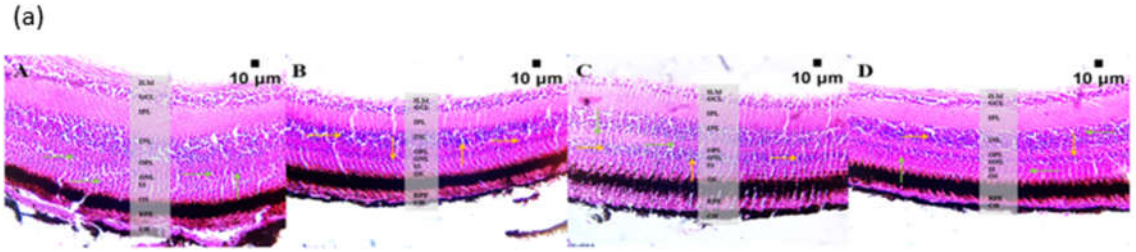

Preprints.org (www.preprints.org) | NOT PEER-REVIEWED | Posted: 10 July 2026 doi:10.20944/preprints202607.0729.v1

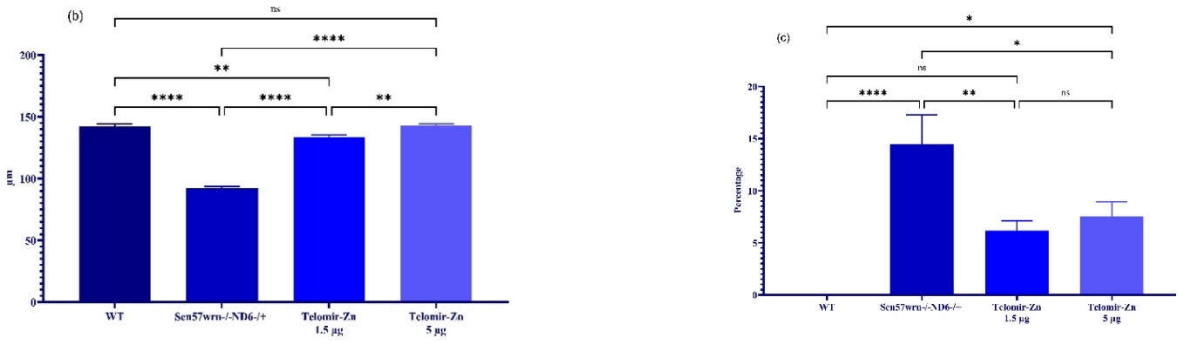

Figure 4. Retinal structural alterations and histological quantification. (**A**) Representative hematoxylin and eosin–stained cross-sections of adult zebrafish retina from wild-type (WT), Sen57$^{wrn-/-}$ND6$^{-/+}$, and treated groups (1.5 μg and 5 μg). Retinal layers are labeled: retinal pigment epithelium (RPE), inner segment (IS), outer segment (OS), photoreceptor layer (PR), outer nuclear layer (ONL), outer plexiform layer (OPL), inner nuclear layer (INL), ganglion cell layer (GCL), and nerve fiber layer (NFL). (**B**) Quantification of overall retinal thickness. (**C**) Percentage of degenerated retinal cells. Data are presented as mean ± SD (n = 6 per group). Statistical analysis was performed using one-way ANOVA followed by Tukey's post hoc test.

2.4.3. Reduction of Mitochondrial Oxidative Stress in an Accelerated Retinal Degeneration Model

Brain ROS levels were quantified as a surrogate measure of mitochondrial oxidative stress, as technical variability limited reliable whole-retina ROS measurements in adult fish [20]. Brain ROS levels were significantly elevated in Sen57$^{wrn-/-}$ND6$^{-/+}$ zebrafish compared with wild-type (WT) controls (3.65 ± 0.44-fold increase; $P < 0.0001$), consistent with mitochondrial dysfunction.

Modulation of intracellular metal homeostasis significantly reduced brain ROS levels at both tested doses, with the higher dose restoring ROS values toward WT baseline ($P < 0.0001$ versus model; Figure 5A).

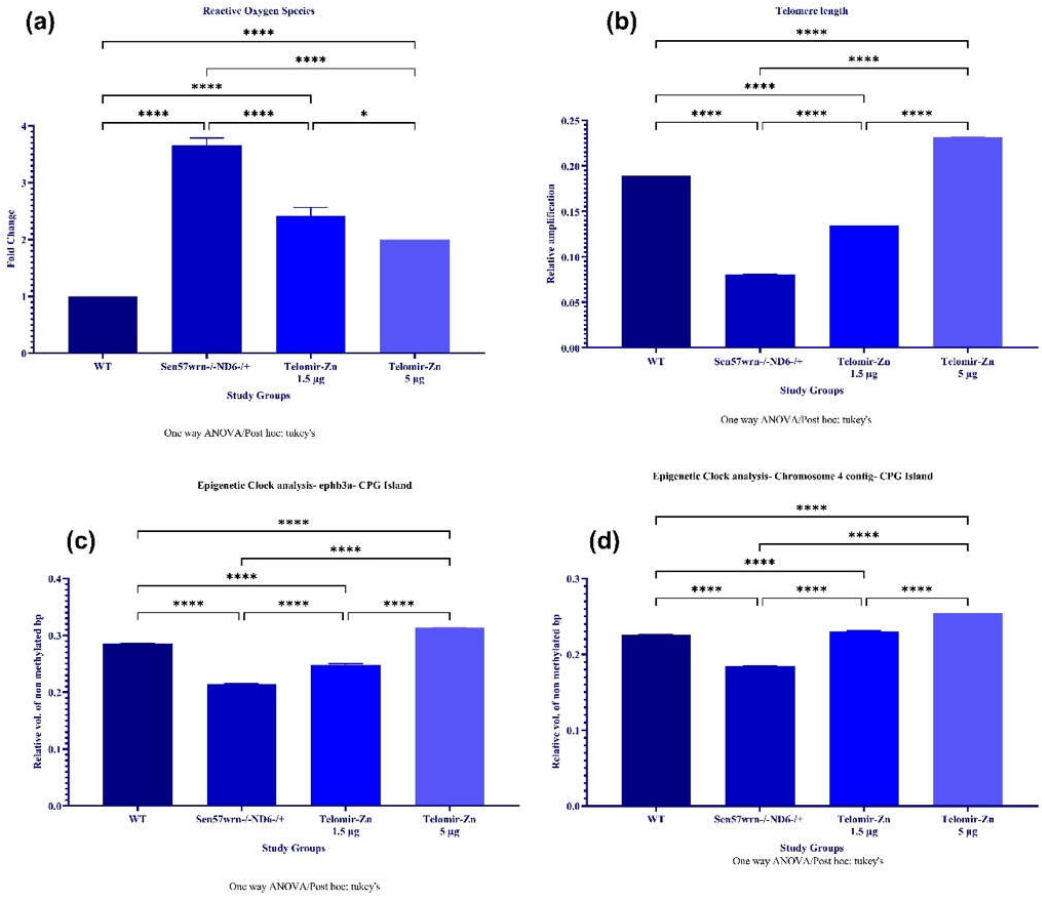

 doi:10.20944/preprints202607.0729.v1

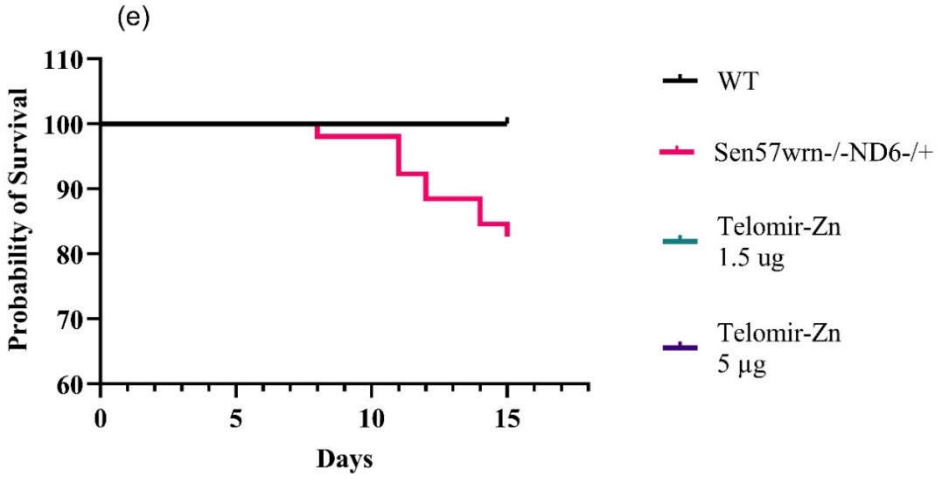

Figure 5. Metal-dependent modulation reduces oxidative stress and alters genomic measures in an accelerated retinal degeneration zebrafish model. (**A**) Brain reactive oxygen species (ROS) levels measured in wild-type (WT), Sen57$^{wrn-/-}$ND6$^{-/+}$, and treated zebrafish. (**B**) Relative telomeric DNA content assessed by PCR-based comparative amplification. (**C**) Relative non-methylated cytosine–phosphate–guanine (CpG) volume at aging-associated loci. (**D**) DNA methylation analysis of chromosome 4 CpG island regions. (**E**) Kaplan–Meier survival curves across experimental groups (n = 52 per group). Data are presented as mean ± SD. Molecular analyses were performed using one-way ANOVA followed by Tukey's post hoc test (n = 12 per group unless otherwise specified). Survival analysis was conducted using the log-rank (Mantel–Cox) test..

2.4.4. Epigenetic and Telomere-Associated Measures

Relative telomeric DNA content was significantly reduced in Sen57$^{wrn-/-}$ND6$^{-/+}$ zebrafish compared with WT controls ($P < 0.0001$). Telomir-Zn treatment was associated with a dose-dependent increase in relative telomeric DNA content (Figure 5B).

DNA methylation analysis at aging-associated cytosine–phosphate–guanine (CpG) loci demonstrated significant alterations in the accelerated degeneration model ($P < 0.0001$). Treatment was associated with partial restoration of methylation patterns at ephb3a and chromosome 4 CpG island regions (Figure 5C,D).

Kaplan–Meier analysis revealed reduced survival in Sen57$^{wrn-/-}$ND6$^{-/+}$ zebrafish (83%) compared with WT controls (100%). Both treated groups exhibited improved survival over the study period (Figure 5E).

2.4.5. Systemic Measures: Body Weight and Muscle Density

Sen57$^{wrn-/-}$ND6$^{-/+}$ zebrafish exhibited reduced body weight and muscle density compared with WT controls. Treatment was associated with increased body weight and improved muscle density relative to the untreated model (Figure 6).

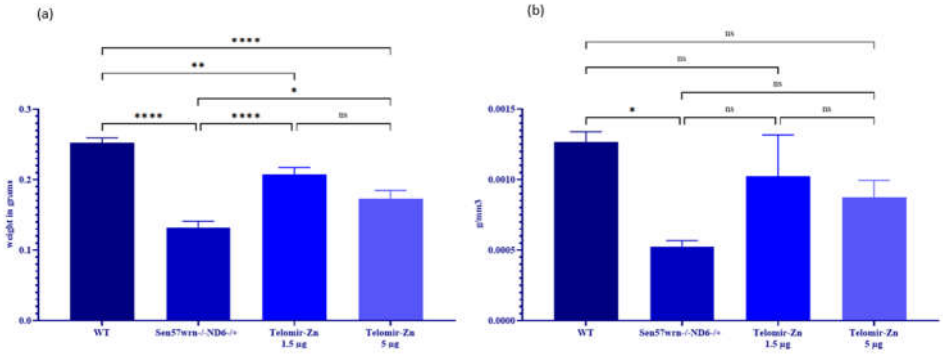

 doi:10.20944/preprints202607.0729.v1

Figure 6. Body weight and muscle density measurements. (**A**) Body weight of adult zebrafish across experimental groups. (**B**) Whole-body density measurements as an indirect indicator of muscle mass. Data are presented as mean ± SD (n = 12 per group). Statistical analysis was performed using one-way ANOVA followed by Tukey's post hoc test.

2.4.6. Blastema Progenitor Cell Volume

Sen57$^{wrn-/-}$ND6$^{-/+}$ zebrafish exhibited reduced blastema progenitor cell volume following caudal fin amputation compared with WT animals ($P < 0.001$). Treatment increased blastema progenitor cell volume at both tested doses (Figure 7).

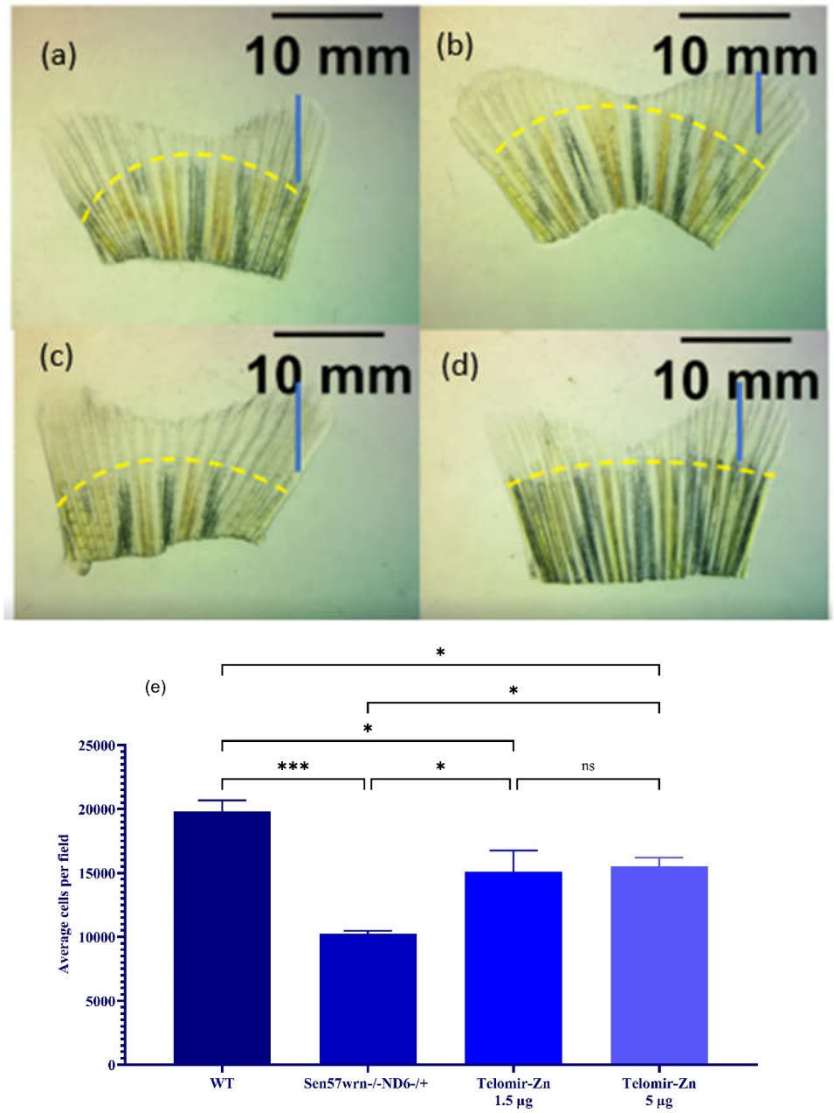

Figure 7. Blastema progenitor cell volume following caudal fin regeneration. (**A**–**D**) Representative stereomicroscopic images of adult zebrafish caudal fins following amputation and regeneration (1× magnification). (**E**) Quantification of blastema progenitor cell volume across experimental groups. Data are presented as mean ± SD (n = 4–6 per group). Statistical analysis was performed using one-way ANOVA followed by Tukey's post hoc test.

3. Discussion

This study demonstrates that modulation of intracellular metal homeostasis reduced oxidative stress and preserved retinal structure and visual performance in a zebrafish model of accelerated retinal degeneration. Across behavioral, histological, molecular, and cellular endpoints, treatment

 doi:10.20944/preprints202607.0729.v1

was associated with improved visual response latency and attenuation of retinal structural disruption.

Iron dysregulation has been increasingly implicated in AMD and other retinal degenerative conditions. Excess labile iron can amplify oxidative injury through Fenton chemistry, promoting lipid peroxidation, mitochondrial dysfunction, and RPE damage. The present findings support the concept that modulation of intracellular redox-active metal balance may represent a complementary strategy for limiting oxidative stress in degenerative retinal disease.

In the accelerated degeneration zebrafish model, ND6 deficiency was associated with elevated brain ROS levels, consistent with mitochondrial dysfunction. Treatment reduced ROS levels toward baseline, suggesting stabilization of redox homeostasis. Although retinal ROS measurements were technically limited in adult animals, complementary cellular studies in human RPE cells demonstrated attenuation of copper- and iron-induced oxidative stress and calcium dysregulation. These findings are consistent with intracellular redistribution of redox-active metal pools rather than simple extracellular chelation.

The observed reciprocal increase in intracellular zinc and reduction in labile ferrous iron suggest that modulation shifts intracellular metal availability toward a less redox-reactive state. Zinc is redox-inert under physiological conditions and serves structural and regulatory roles in numerous proteins. Increasing intracellular zinc while reducing labile Fe^{2+} may decrease susceptibility to oxidative stress without broadly disrupting essential metal-dependent processes.

Improvements in visual response latency were accompanied by reduced structural disruption of the outer nuclear layer and photoreceptor compartments. The concordance between behavioral and histological findings supports the possibility that metal-dependent redox modulation influences retinal tissue integrity under conditions of mitochondrial stress.

Alterations in DNA methylation patterns and relative telomeric DNA content were observed in the accelerated degeneration model and were modified following treatment. Although the functional implications of these genomic measures require further investigation, iron-dependent chromatin-modifying enzymes are sensitive to intracellular redox state and metal availability. These findings suggest that modulation of redox-active metals may influence broader cellular stress-response pathways relevant to retinal degeneration.

Systemic measures, including body weight, muscle density, and blastema progenitor cell volume, were also modified following treatment. These findings should be interpreted cautiously, and further studies will be necessary to determine tissue specificity and relevance to retinal disease.

Several limitations of the present study should be acknowledged. First, the treatment duration was relatively short (14 days). While this timeframe was sufficient to demonstrate rapid improvements in visual function, retinal structural preservation, and reduction of oxidative stress, longer-term studies will be necessary to evaluate the durability of these protective effects and potential disease-modifying benefits over extended periods of degeneration.

Second, due to technical constraints associated with reliable ROS measurement in the small retinal tissue of adult zebrafish, we used brain ROS levels as a surrogate marker of mitochondrial oxidative stress. However, the complementary in vitro data in human ARPE-19 retinal pigment epithelial cells, which directly demonstrated dose-dependent attenuation of both iron- and copper-induced ROS production and calcium dysregulation, strongly support the translational relevance of reduced oxidative burden in retinal cells.

Third, although the Sen57$^{wrn-/-}$ND6$^{-/+}$ zebrafish line effectively recapitulates key pathological features of oxidative stress, mitochondrial dysfunction, and accelerated retinal degeneration relevant to human AMD, it does not fully model the complex, chronic, and multifactorial nature of age-related macular degeneration in humans. Additional validation in mammalian models of retinal degeneration (e.g., iron-overload or photo-oxidative damage models) will be important to further establish therapeutic potential.

The potent multi-KDM inhibitory profile of Telomir-Zn provides a direct mechanistic link between intracellular Fe^{2+} depletion and the observed reductions in oxidative stress, partial

 doi:10.20944/preprints202607.0729.v1

normalization of CpG methylation and telomeric content, and preservation of retinal structure/function. By inhibiting Fe^{2+}-dependent demethylases such as KDM5B and KDM6B—implicated in senescence, inflammation, and oncogenic/stress programs—Telomir-Zn likely promotes a more protective epigenetic landscape in RPE and photoreceptors under oxidative burden [23].

These findings extend the therapeutic paradigm of metal modulation from oncology (where KDM inhibition suppresses tumor growth via epigenetic reprogramming) to retinal degeneration, highlighting a conserved vulnerability at the intersection of metal homeostasis, redox balance, and chromatin regulation.

Finally, while treatment was associated with partial normalization of relative telomeric DNA content and select CpG methylation patterns, the functional consequences of these epigenetic changes on photoreceptor survival and RPE integrity remain to be fully elucidated. Future mechanistic studies will be required to establish causal relationships between intracellular metal redistribution, epigenetic regulation, and long-term retinal protection.

Despite these limitations, the multi-level convergence of behavioral, histological, cellular, and molecular findings provides compelling proof-of-concept that modulation of intracellular metal homeostasis represents a promising strategy for mitigating oxidative retinal damage.

In summary, modulation of intracellular redox-active metal balance was associated with reduced oxidative stress and preservation of retinal structure and visual performance in a vertebrate model of retinal degeneration. These findings are consistent with a model in which intracellular metal redistribution stabilizes mitochondrial redox homeostasis and may influence genomic regulatory pathways that contribute to retinal integrity (Figure 8).

Figure 8. Proposed model linking redox-active metal dysregulation to retinal oxidative stress and degeneration. Schematic representation of a proposed mechanism whereby expansion of intracellular labile iron and copper pools increases mitochondrial reactive oxygen species (ROS) production, contributing to oxidative stress and impaired retinal integrity. Modulation of intracellular metal balance is proposed to reduce redox-active metal availability and stabilize mitochondrial redox homeostasis.

4. Materials and Methods

4.1. Telomir-Zn

Telomir-Zn is a zinc-complexed small molecule consisting of 2,4,6-tris(3,4-dihydro-2H-pyrrol-2-yl)pyridine coordinated with $ZnCl_2$. The compound was synthesized by Recipharm (Israel) and supplied at a purity of 95%.

4.2. Cell Culture

ARPE-19 human retinal pigment epithelial cells (ATCC CRL-2302) and HaCaT human keratinocytes (AddexBio T0020001) were cultured in Dulbecco's Modified Eagle Medium/Ham's F-12 (DMEM/F12; Biowest, L0093) and DMEM (Biowest, L0102), respectively. Media were supplemented with 10% fetal bovine serum (FBS; Gibco, A5256701) and 1% penicillin–streptomycin (Gibco, 15140-122). HaCaT cultures were additionally supplemented with 2 mM sodium pyruvate (Sartorius, 03-042-1B).

Cells were maintained at 37 °C in a humidified incubator with 5% CO_2. ARPE-19 and HaCaT cells were seeded into 96-well plates at densities of 20,000 and 10,000 cells per well, respectively. Experiments were performed 2–5 days after seeding at approximately 90% confluence.

4.3. Reactive Oxygen Species (ROS) Assay

Cells were incubated with Telomir-Zn at final concentrations of 0.1, 0.5, 1, or 5 μM in complete culture medium, with or without copper chloride ($CuCl_2$; 25 μM; Sigma, C3279), for 24 h at 37 °C.

 doi:10.20944/preprints202607.0729.v1

Following incubation, cells were washed twice with Hanks' Balanced Salt Solution (HBSS) and stained with 2′,7′-dichlorofluorescein diacetate (DCFH-DA) for 2 h at 37 °C. Fluorescence was measured using a microplate reader (CLARIOstar, BMG Labtech).

Cell viability was assessed in parallel using the WST-1 assay (Sigma-Aldrich, 5015944001) according to the manufacturer's instructions. Reactive oxygen species (ROS) values were normalized to cell viability.

4.4. Calcium Flux Assay

Cells were incubated with Telomir-Zn at final concentrations of 0.1, 0.5, 1, or 5 μM for 1 hour at 37 °C. Cells were then washed and equilibrated in assay buffer consisting of HBSS supplemented with 0.1 mM calcium chloride ($CaCl_2$), 0.9 mM magnesium chloride ($MgCl_2$), and 20 mM HEPES.

Cells were loaded with the calcium-sensitive fluorescent dye Fluo-8 (AAT Bioquest, 21081) in the presence of probenecid (Sigma, P8761) for 1 h at 37 °C. Telomir-Zn was maintained at designated concentrations during dye loading.

Following dye loading, cells were challenged with Cu^{2+} (25 μM) or Fe^{2+} (10 μM). Fluorescence intensity was recorded at 2-minute intervals for 40 min using a microplate reader.

4.5. Intracellular Zinc and Iron Fluorescence Imaging

HaCaT cells were seeded into 96-well plates and maintained as described above.

For zinc detection, cells were incubated with Telomir-Zn (0.01–5 μM) for 2 h at 37 °C and stained with DA-ZP1 (1 μM; R&D Systems, 7444/2) for 30 minutes. Cells were washed twice with HBSS prior to imaging.

For labile ferrous iron detection, cells were incubated with Telomir-Zn (0.01–5 μM) for 2 hours and stained with FerroOrange (1 μM; Dojindo, F374) for 30 minutes at 37 °C.

Fluorescence imaging was performed using a fluorescence microscope at 10× magnification. DA-ZP1 was imaged with excitation at 480 nm and emission collected using a 510–550 nm band-pass filter. FerroOrange was imaged with excitation at 545 nm and emission collected using a 575–650 nm band-pass filter.

4.6. Histone Demethylase (KDMs) Assay

The inhibitory activity of Telomir-Zn against recombinant JmjC-domain histone demethylases was evaluated using established biochemical assays as previously described [21,22].

Briefly, Sf9 insect cells were used to express individual human recombinant KDM enzymes (KDM2, KDM5, and KDM6 family members). Enzyme activity was measured in the presence of varying concentrations of Telomir-Zn using biotinylated histone peptide substrates specific to each family:

Biotin-H3K36me1 for KDM2 enzymes, Biotin-H3K4me2 for KDM5 enzymes, and Biotin-H3K27me2 for KDM6 enzymes. Demethylation reactions were quantified by detecting the release of formaldehyde or through antibody-based detection of remaining methyl marks. IC_{50} values were determined from dose-response curves performed in duplicate or triplicate.

4.7. Zebrafish Husbandry and Ethics

Wild-type and genetically modified zebrafish (*Danio rerio*) were bred and maintained at the Pentagrit Discovery facility under standard laboratory conditions (27 ± 1 °C; pH 7.2–7.4; 14-hour light/10-hour dark cycle). Fish were fed commercial flake food twice daily.

All experimental procedures adhered to the ARVO Statement for the Use of Animals in Ophthalmic and Vision Research. Studies were conducted at an AAALAC International–accredited facility and were reviewed and approved by the Institutional Animal Ethics Committee (IAEC). All protocols complied with the guidelines of the Committee for the Control and Supervision of Experiments on Animals (CCSEA), Government of India. Ethical approval number: PENT014.

 doi:10.20944/preprints202607.0729.v1

4.8. Accelerated Retinal Degeneration Zebrafish Model

An accelerated degeneration zebrafish line (Sen57$^{wrn-/-}$ND6$^{-/+}$) was generated using N-ethyl-N-nitrosourea (ENU) mutagenesis followed by selective inbreeding. This model combines deficiency of Werner syndrome helicase (*wrn*) with mitochondrial electron transport chain dysfunction resulting from *ND6* mutation.

Heterozygous founders were intercrossed to generate mutants. Adult zebrafish were aged to 18 months prior to experimental intervention.

4.9. Experimental Groups and Treatment Administration

Adult zebrafish were allocated to experimental groups following genotypic confirmation. Each group consisted of 52 biologically independent animals.

Four groups were studied:

1. Wild-type (WT)
2. Sen57$^{wrn-/-}$ND6$^{-/+}$ mutants
3. Sen57$^{wrn-/-}$ND6$^{-/+}$ treated with Telomir-Zn (1.5 µg)
4. Sen57$^{wrn-/-}$ND6$^{-/+}$ treated with Telomir-Zn (5 µg)

Telomir-Zn was administered orally once daily for 14 days via compound-infused pellets. Housing water was refreshed every 24 h.

4.10. Visual and Behavioral Assessments

Visual function was evaluated using assays assessing central visual response, moving object tracking, and adaptation to changes in light intensity. Individual fish were acclimated prior to stimulus presentation. Latency to response was defined as the time from stimulus onset to initiation of directed motor behavior.

4.11. Histological Analysis

Following 14 days of treatment, adult zebrafish (n = 6 per group) were euthanized, and eyes were dissected and fixed in 5% neutral buffered formalin for 48 h. Tissues were dehydrated, cleared, and embedded in paraffin.

Paraffin sections (10 µm) were stained with hematoxylin and eosin (H&E). Images were captured using light microscopy. Quantification of retinal degeneration was performed using QuPath software in a masked manner. Degeneration percentage was calculated as degenerated cells divided by total cells × 100.

4.12. Reactive Oxygen Species Measurement in Zebrafish Brain

Brain ROS levels were quantified using a fluorometric assay (ROS Detection Kit; Sigma-Aldrich, MAK143). Brains (n = 12 per group) were isolated and homogenized in assay buffer. Total protein concentration was determined, and equal amounts of protein were used for each reaction.

Samples were incubated with detection reagent for 30 min at 37 °C. Fluorescence was measured at excitation/emission 490/525 nm. Values were normalized to total protein content.

4.13. DNA Methylation Analysis

Genomic DNA was isolated from fin tissue (n = 6 per group, pooled in pairs) using a silica column–based kit (QIAamp Mini Kit, Qiagen). DNA was subjected to sodium bisulfite conversion followed by locus-specific amplification.

Target loci included ephb3a and selected chromosome 4 CpG island regions. Amplified products were analyzed comparatively across groups.

4.14. Relative Telomeric DNA Content

 doi:10.20944/preprints202607.0729.v1

Relative telomeric DNA content was assessed using a PCR-based comparative amplification method. Genomic DNA was amplified in triplicate under identical reaction conditions. Amplification products were resolved on agarose gels and quantified by densitometric analysis. Relative telomeric content was calculated based on comparative amplification intensity across groups.

4.15. Survival Analysis

Mortality was recorded daily throughout the 14-day treatment period. Survival curves were generated using the Kaplan–Meier method. Differences between groups were evaluated using the log-rank (Mantel–Cox) test. No animals were censored during the study period.

4.16. Statistical Analysis

Statistical analyses were performed using GraphPad Prism (version 10; GraphPad Software, San Diego, CA, USA). Data are presented as mean ± standard deviation (SD). Comparisons among multiple groups were performed using one-way analysis of variance (ANOVA) followed by Tukey's multiple-comparisons post hoc test, unless otherwise specified. Survival curves were analyzed using the Kaplan–Meier method with group comparisons performed using the log-rank (Mantel–Cox) test.

All analyses were conducted using biologically independent samples. Sample sizes for each experiment are indicated in the corresponding figure legends. All tests were two-tailed, and a P value < 0.05 was considered statistically significant.

5. Conclusions

Modulation of intracellular redox-active metal balance was associated with reduced oxidative stress and preservation of retinal structure and visual performance in a zebrafish model of accelerated retinal degeneration. Complementary cellular studies in human RPE cells demonstrated attenuation of iron- and copper-induced oxidative stress and calcium dysregulation.

These findings support a role for metal-dependent regulation of mitochondrial redox homeostasis in retinal degenerative processes. Given the established contribution of oxidative stress and altered iron handling to age-related macular degeneration, targeted modulation of intracellular metal balance merits further investigation in mammalian models of retinal disease.

Author Contributions: I.A. and E.A. conceived and designed the study. M.G. performed the in vitro experiments under the supervision of R.M. K.P. and B.J. conducted the in vivo zebrafish experiments. I.A. and E.A. analyzed and interpreted the data. I.A. drafted the manuscript. All authors have read and agreed to the published version of the manuscript.

Funding: This work was funded by Telomir Pharmaceuticals, Inc.

Institutional Review Board Statement: The animal study protocol was approved by the Institutional Animal Ethics Committee (IAEC) and conducted at an AAALAC International–accredited facility in compliance with the guidelines of the Committee for the Control and Supervision of Experiments on Animals (CCSEA), Government of India, and the ARVO Statement for the Use of Animals in Ophthalmic and Vision Research (approval code PENT014).

Informed Consent Statement: Not applicable.

Data Availability Statement: The data supporting the findings of this study are included within the article and its supplementary materials. Additional data are available from the corresponding author. ChatGPT, Claude, and Grok were used for the verification of abbreviations, references, adherence to journal requirements, and for the production of Figure 8 of the manuscript.

Acknowledgments: The authors thank the scientific and technical staff at Pentagrit Discovery for assistance with the in vivo experiments and Smart Assays Biotechnologies for support with cellular studies.

 doi:10.20944/preprints202607.0729.v1

Conflicts of Interest: E.A. is Chief Executive Officer of Telomir Pharmaceuticals, Inc. I.A. serves as a consultant to Telomir Pharmaceuticals, Inc. Telomir Pharmaceuticals, Inc. is developing Telomir-1. Telomir-Zn, the compound evaluated in this study and advanced in clinical trials, is a zinc complex of Telomir-1 (Telomir-1 coordinated with $ZnCl_2$). The remaining authors declare no competing financial interests.

Abbreviations

The following abbreviations are used in this manuscript:

AAALAC	Association for Assessment and Accreditation of Laboratory Animal Care International
AMD	Age-related macular degeneration
ANOVA	Analysis of variance
CCSEA	Committee for the Control and Supervision of Experiments on Animals
CpG	Cytosine–phosphate–guanine
DCFH-DA	2′,7′-Dichlorofluorescein diacetate
DNA	Deoxyribonucleic acid
ENU	N-ethyl-N-nitrosourea
FBS	Fetal bovine serum
Fe^{2+}	Ferrous iron
GCL	Ganglion cell layer
H&E	Hematoxylin and eosin
HBSS	Hanks' Balanced Salt Solution
IAEC	Institutional Animal Ethics Committee
IC_{50}	Half-maximal inhibitory concentration
INL	Inner nuclear layer
JmjC	Jumonji C
KDM	Lysine (K) demethylase
NFL	Nerve fiber layer
ONL	Outer nuclear layer
OPL	Outer plexiform layer
OS	Outer segment
PCR	Polymerase chain reaction
PR	Photoreceptor layer
ROS	Reactive oxygen species
RPE	Retinal pigment epithelium
SD	Standard deviation
WST-1	Water-soluble tetrazolium salt-1
WT	Wild-type

References

1. Ferrington, D.A.; Fisher, C.R.; Kowluru, R.A. Mitochondrial Defects Drive Degenerative Retinal Diseases. *Trends Mol. Med.* **2020, 26**, 105–118. doi:10.1016/j.molmed.2019.10.008.
2. Bibliowicz, J.; Tittle, R.K.; Gross, J.M. Toward a Better Understanding of Human Eye Disease: Insights from the Zebrafish, *Danio rerio*. *Prog. Mol. Biol. Transl. Sci.* **2011, 100**, 287–330. doi:10.1016/B978-0-12-384878-9.00007-8.
3. Valko, M.; Morris, H.; Cronin, M.T.D. Metals, Toxicity and Oxidative Stress. *Curr. Med. Chem.* **2005, 12**, 1161–1208. doi:10.2174/0929867053764635.
4. Dentchev, T.; Hahn, P.; Dunaief, J.L. Strong Labeling for Iron and the Iron-Handling Proteins Ferritin and Ferroportin in the Photoreceptor Layer in Age-Related Macular Degeneration. *Arch. Ophthalmol.* **2005, 123**, 1745–1746. doi:10.1001/archopht.123.12.1745.
5. Galaris, D.; Barbouti, A.; Pantopoulos, K. Iron Homeostasis and Oxidative Stress: An Intimate Relationship. *Biochim. Biophys. Acta Mol. Cell Res.* **2019, 1866**, 118535. doi:10.1016/j.bbamcr.2019.118535.
6. Liu, J.; Kuang, F.; Kroemer, G.; Klionsky, D.J.; Kang, R.; Tang, D. Autophagy-Dependent Ferroptosis: Machinery and Regulation. *Cell Chem. Biol.* **2020, 27**, 420–435. doi:10.1016/j.chembiol.2020.02.005.

 doi:10.20944/preprints202607.0729.v1

7. Hausinger, R.P. FeII/α-Ketoglutarate-Dependent Hydroxylases and Related Enzymes. *Crit. Rev. Biochem. Mol. Biol.* **2004, 39**, 21–68. doi:10.1080/10409230490440541.
8. Kooistra, S.M.; Helin, K. Molecular Mechanisms and Potential Functions of Histone Demethylases. *Nat. Rev. Mol. Cell Biol.* **2012, 13**, 297–311. doi:10.1038/nrm3327.
9. Corso-Díaz, X.; Jaeger, C.; Chaitankar, V.; Swaroop, A. Epigenetic Control of Gene Regulation During Development and Disease: A View from the Retina. *Prog. Retin. Eye Res.* **2018, 65**, 1–27. doi:10.1016/j.preteyeres.2018.03.002.
10. Johansson, C.; Tumber, A.; Che, K.; Cain, P.; Nowak, R.; Gileadi, C.; Oppermann, U. The Roles of Jumonji-Type Oxygenases in Human Disease. *Epigenomics* **2014, 6**, 89–120. doi:10.2217/epi.13.79.
11. Maret, W. Zinc in Cellular Regulation: The Nature and Significance of Zinc Signals. *Int. J. Mol. Sci.* **2017, 18**, 2285. doi:10.3390/ijms18112285.
12. Krężel, A.; Maret, W. The Biological Inorganic Chemistry of Zinc Ions. *Arch. Biochem. Biophys.* **2016, 611**, 3–19. doi:10.1016/j.abb.2016.04.010.
13. Cassandri, M.; Smirnov, A.; Novelli, F.; Pitolli, C.; Agostini, M.; Malewicz, M.; Melino, G.; Raschellà, G. Zinc-Finger Proteins in Health and Disease. *Cell Death Discov.* **2017, 3**, 17071. doi:10.1038/cddiscovery.2017.71.
14. Howe, K.; Clark, M.D.; Torroja, C.F.; Torrance, J.; Berthelot, C.; Muffato, M.; et al. The Zebrafish Reference Genome Sequence and Its Relationship to the Human Genome. *Nature* **2013, 496**, 498–503. doi:10.1038/nature12111.
15. George, S.M.; Lu, F.; Rao, M.; Leach, L.L.; Gross, J.M. The Retinal Pigment Epithelium: Development, Injury Responses, and Regenerative Potential in Mammalian and Non-Mammalian Systems. *Prog. Retin. Eye Res.* **2021, 85**, 100969. doi:10.1016/j.preteyeres.2021.100969.
16. Lebel, M.; Leder, P. A Deletion Within the Murine Werner Syndrome Helicase Induces Sensitivity to Inhibitors of Topoisomerase and Loss of Cellular Proliferative Capacity. *Proc. Natl. Acad. Sci. U.S.A.* **1998, 95**, 13097–13102. doi:10.1073/pnas.95.22.13097.
17. Eichenbaum, J.W.; Cinaroglu, A.; Eichenbaum, K.D.; Sadler, K.C. A Zebrafish Retinal Graded Photochemical Stress Model. *J. Pharmacol. Toxicol. Methods* **2009, 59**, 121–127. doi:10.1016/j.vascn.2009.02.006.
18. Wallace, D.C. Mitochondrial DNA Mutations in Disease and Aging. *Environ. Mol. Mutagen.* **2010, 51**, 440–450. doi:10.1002/em.20586.
19. Ma, J., Chen, Y.; et al. Establishment and Application of a Zebrafish Model of Werner Syndrome Identifies Sapanisertib as a Potential Antiaging Drug. *Proc. Natl. Acad. Sci. U.S.A.* **2025, 122**, e2413719122. doi:10.1073/pnas.2413719122.
20. White, R.M.; Sessa, A.; Burke, C.; Bowman, T.; LeBlanc, J.; Ceol, C.; Bourque, C.; Dovey, M.; Goessling, W.; Burns, C.E.; Zon, L.I. Transparent Adult Zebrafish as a Tool for In Vivo Transplantation Analysis. *Cell Stem Cell* **2008, 2**, 183–189. doi:10.1016/j.stem.2007.11.002.
21. Grubwieser, P.; Brigo, N.; Seifert, M.; Grander, M.; Theurl, I.; Nairz, M.; Weiss, G.; Pfeifhofer-Obermair, C. Quantification of Macrophage Cellular Ferrous Iron (Fe^{2+}) Content Using a Highly Specific Fluorescent Probe in a Plate Reader. *Bio Protoc.* **2024, 14**, e4929. doi:10.21769/BioProtoc.4929.
22. Kristensen, L.H.; Nielsen, A.L.; Helgstrand, C.; Lees, M.; Cloos, P.; Kastrup, J.S.; Helin, K.; Olsen, L.; Gajhede, M. Studies of H3K4me3 Demethylation by KDM5B/Jarid1B/PLU1 Reveals Strong Substrate Recognition In Vitro and Identifies 2,4-Pyridine-Dicarboxylic Acid as an In Vitro and In Cell Inhibitor. *FEBS J.* **2012, 279**, 1905–1914. doi:10.1111/j.1742-4658.2012.08567.x.
23. Rajanala, K.; Upadhyay, A. Epigenetic Switches in Retinal Homeostasis and Target for Drug Development. *Int. J. Mol. Sci.* **2024, 25**, 2840. doi:10.3390/ijms25052840.